Numerical studies of fast pressure crash associated with double tearing modes

W. Zhang[1], Z. W. Ma[1,*], and H. W. Zhang[1]

[1]Institute for Fusion Theory and Simulation, Department of Physics, Zhejiang University, Hangzhou 310027, China

Abstract: The fast pressure crash associated with the nonlinear evolution of DTMs is investigated using a three-dimensional toroidal and nonlinear MHD code CLT. It is found that dependence of the pressure crash time on the resistivity is much weaker than that in previous studies, and the pressure crash begins when the explosive mode growth almost finishes. It is also found that the pressure crash time is nearly independent of the parallel thermal conductivity. The fast pressure crash is mainly resulted from generation of the outward radial flow when magnetic field lines in the core region become stochastic due to magnetic reconnection. The radial flow can effectively transfer the hot plasma around the magnetic axis into the outer region. With TFTR parameters, the crash time is about 36 μs that agrees well with that from TFTR observations (20~40 μs). It is also found that the Tokamak geometry does not influence the time scale of the pressure crash.

*The corresponding author: zwma@zju.edu.cn

I. Introduction

In present Tokamaks (such as DIII-D[1], TFTR[2], NSTX[3],ASDEX-U[4], JET[5],and TPX[6]), it is found that the negative magnetic shear in the core region can help to suppress the drift instabilities[6], stabilize ballooning mode instabilities[7], suppress Electron Temperature Gradient Turbulence[3] and then significantly improve plasma confinement. Due to its advantage in the superior energy confinement, the reversed magnetic shear configuration has been adopted as one of the advanced scenarios in future fusion reactors such as ITER[8, 9] and CFETR[10]. However, there exists a destructive non-ideal instability, i. e. Double Tearing Mode (DTM) in such configuration.[11-31] In the linear phase, DTM grows much faster than a single tearing mode because two tearing modes with the same helicity on the resonant surfaces could strongly couple with each other. The nonlinear evolution of DTM can result in an off-axis sawtooth or a core-crash sawtooth, which can greatly degrade energy confinement in Tokamak.[3, 32, 33] During an off-axis sawtooth, the temperature crash only takes place in the annular region, while the temperature around the magnetic axis remains almost unchanged. However, during a core-crash sawtooth, the temperature becomes flattened in a broad region (including the magnetic axis).

It is widely accepted that core crash sawteeth observed in TFTR are closely related to the nonlinear evolution of the $m/n=2/1$ DTM, where *m* and *n* are the poloidal and toroidal mode numbers, respectively. However, the physical mechanism for the fast pressure crash is still in debate. [27, 28, 34-43] The pressure crash time observed in TFTR is about 20~40 μs, [32] but the crash time shown in Chang's simulation corresponds to the Sweet-Parker[44] reconnection time $\tau_R^{1/2}\tau_A^{1/2}$ (where τ_R is the resistive diffusion time and τ_A is the Alfvén time), which is ~1 ms for TFTR parameters.[32] Ishii et al. [35] and Janvier et al. [36] found that the explosive nonlinear growth of the DTM is triggered when the triangular deformation of magnetic islands with a sharp current point at the X point exceeds a critical value. Therefore, they suggested it is a structure driven mode. Wang et al. [38] found that the growth rate in the crash phase is $\sim\eta^{1/5}$ (where η is the resistivity), which is the same with the flow driven reconnection[45].

In the present paper, a series of numerical simulations are conducted using a three-dimensional toroidal MHD code CLT.[46] It is found that the pressure crash time is nearly independent of the resistivity. With TFTR parameters [2, 32], the crash time in our simulations is about 36 μs, which is consistent with experimental observations (20~40 μs). It should be noted that, in previous studies,[34, 36, 38, 47] the fast pressure crash occurs together with the explosive growth of the modes. However, as shown in the present paper, the pressure crash occurs about one hundred of Alfvén times after the explosive growth of the modes. It also should be noted that the crash time is independent of the parallel thermal conductivity, which indicates that the fast pressure crash is not directly driven from the fast reconnection of the magnetic field.

II. Model description

The model used in CLT is the single-fluid MHD model (Eq. (1.1)~(1.6)).

$$\frac{\partial \rho}{\partial t} = -\nabla\cdot(\rho\mathbf{v}) + \nabla\cdot[D\nabla(\rho)] \tag{1.1}$$

$$\frac{\partial p}{\partial t} = -\mathbf{v}\cdot\nabla p - \Gamma p\nabla\cdot\mathbf{v} + \nabla\cdot[\kappa_{\perp}\nabla(p-p_0)] + \nabla\cdot[\kappa_{\parallel}\nabla_{\parallel} p] \tag{1.2}$$

$$\frac{\partial \mathbf{v}}{\partial t} = -\mathbf{v}\cdot\nabla\mathbf{v} + (\mathbf{J}\times\mathbf{B} - \nabla p)/\rho + \nabla\cdot[\nu\nabla(\mathbf{v})] \tag{1.3}$$

$$\frac{\partial \mathbf{B}}{\partial t} = -\nabla\times\mathbf{E} \tag{1.4}$$

$$\mathbf{E} = -\mathbf{v}\times\mathbf{B} + \eta(\mathbf{J}-\mathbf{J}_0) \tag{1.5}$$

$$\mathbf{J} = \nabla\times\mathbf{B} \tag{1.6}$$

where ρ, p, $\mathbf{v}$, $\mathbf{B}$, $\mathbf{E}$, and $\mathbf{J}$ are the plasma density, the plasma pressure, the velocity, magnetic field, the electric field, and the current density, respectively. The subscript "0" denotes the initial quantities. $\Gamma(=5/3)$ is the ratio of specific heat of the plasma.

B_0 and ρ_{00} are the magnetic field and the plasma density at the magnetic axis, respectively. All variables in CLT are normalized as follows: $\mathbf{x}/a \to \mathbf{x}$, $\rho/\rho_{00} \to \rho$, $p/(B_0^2/\mu_0) \to p$, $t/t_A \to t$, $\mathbf{v}/v_A \to \mathbf{v}$, $\mathbf{B}/B_0 \to \mathbf{B}$, $\mathbf{E}/(v_A B_0) \to \mathbf{E}$, and $\mathbf{J}/(B_0/\mu_0 a) \to \mathbf{J}$ where a is the minor radius, $v_A = B_0/\sqrt{\mu_0\rho_{00}}$ is the Alfvén speed, and $t_A = a/v_A$ is the Alfvén time. The resistivity η and the diffusion coefficient D, the perpendicular and parallel thermal conductivity $\kappa_\perp$ and $\kappa_\parallel$, the viscosity ν are normalized as follows: $\eta/(\mu_0 a^2/t_A) \to \eta$, $D/(a^2/t_A) \to D$, $\kappa_\perp/(a^2/t_A) \to \kappa_\perp$, $\kappa_\parallel/(a^2/t_A) \to \kappa_\parallel$, and $\nu/(a^2/t_A) \to \nu$, respectively.

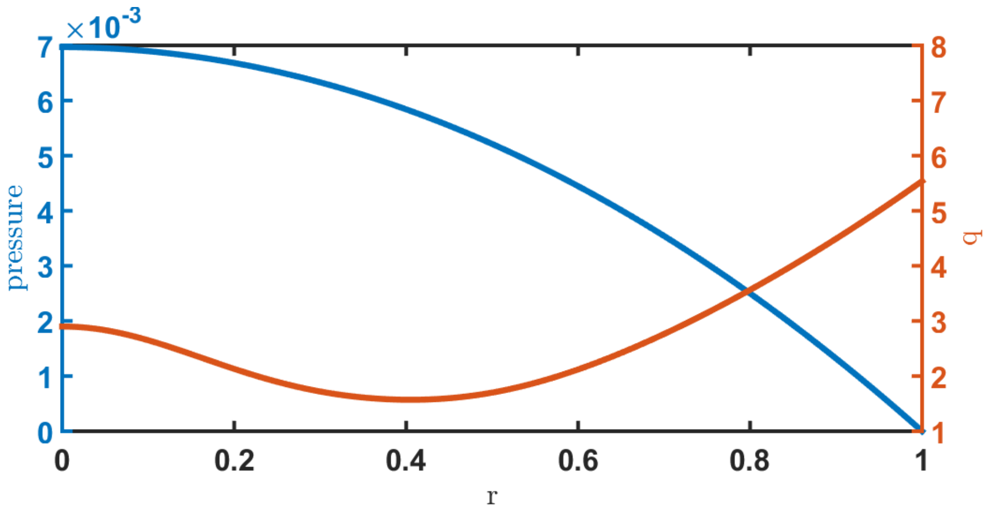

Figure 1 Initial pressure profile and q profile.

For TFTR [2, 32], the major and minor radiuses are $R_0 = 2.60m$ and $a = 0.94m$, respectively. The toroidal field $B_0 \sim 4.2T$, the electron density $n_e \sim 1.0\times10^{20} m^3$, and electron temperature $T_e \sim 5kev$. The corresponding resistivity $\eta \sim 1\times10^{-9}$ and the Alfvén time $t_A = 1.08\times10^{-7} s$. Due to the limit of computational capability, the resistivity used in the present paper is from $\eta \sim 1\times10^{-5}$ to $\eta \sim 1\times10^{-7}$. We will show that the crash time is almost independent of the resistivity, then the value of the resistivity will not be an issue.

III. Simulation results

The initial pressure profile and the q profile are shown in Figure 1. The plasma beta and the q-value at the magnetic axis are set to be $\beta_0 = 1.4\%$ and $q_0 = 2.9$, respectively. As there are two q=2 resonant surfaces, the m/n=2/1 DTM is the most unstable mode in this system. The equilibrium is obtained from the NOVA code.[48] The grids used in the simulations are $256 \times 32 \times 256\ (R, \varphi, Z)$, and convergence studies have been ensured by verifying the time step and spatial resolution. The normalized parameters for the typical case are $D = 1.0 \times 10^{-4}$, $\kappa_{\perp} = 5.0 \times 10^{-6}$, $\kappa_{\parallel} = 5.0 \times 10^{-2}$, $\upsilon = 1.0 \times 10^{-5}$, and $\eta = 1.0 \times 10^{-7}$, respectively.

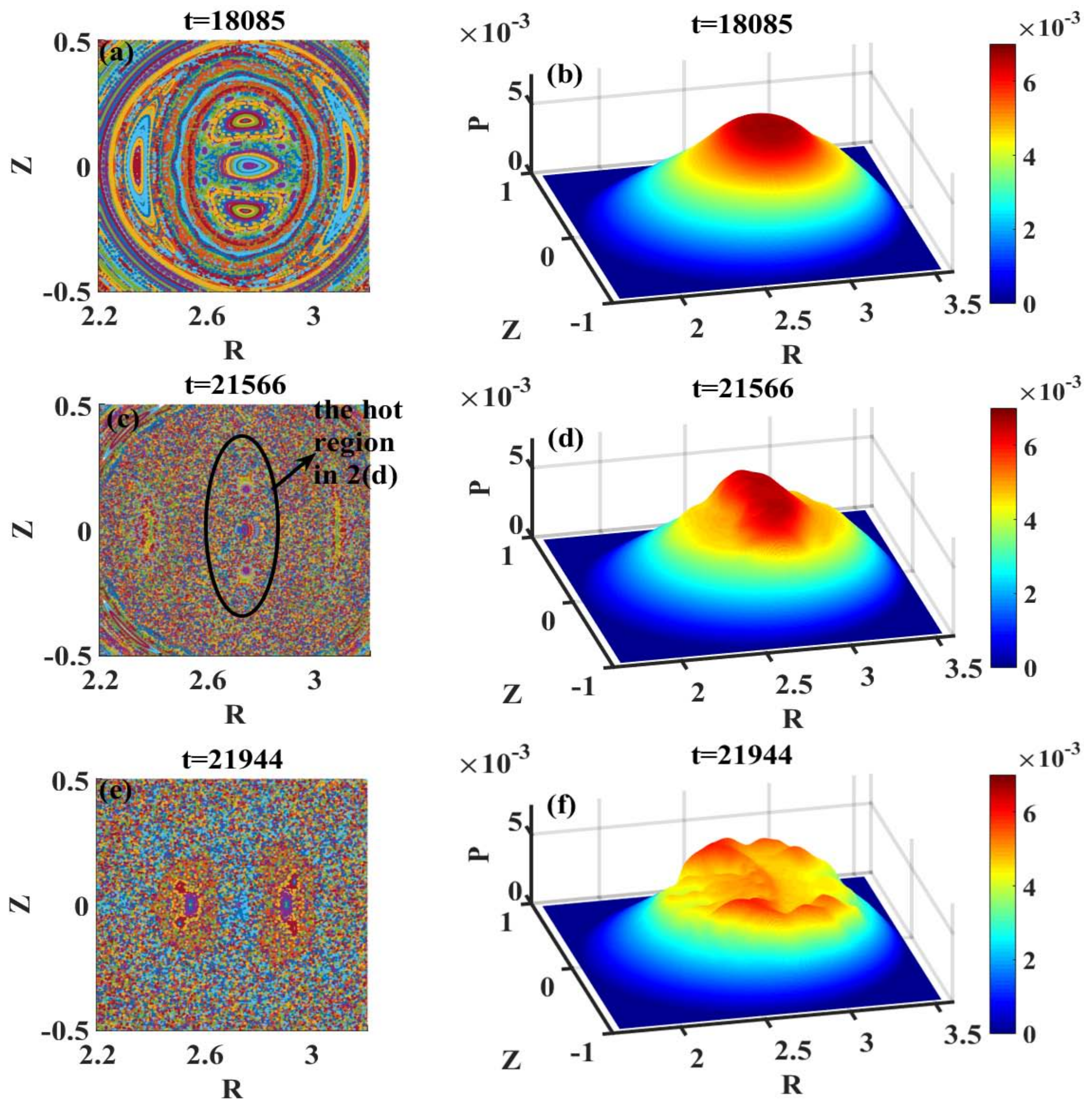

Figure 2 Poincare plots of magnetic field lines and pressure distributions at the precursor ($t = 18085 t_A$), at the pre-crash ($t = 21566 t_A$), and the post-crash ($t = 21944 t_A$) of the core-crash sawtooth.

Poincare plots of magnetic field lines and pressure distributions at the precursor ($t = 18085 t_A$), the pre-crash ($t = 21566 t_A$), and the post-crash ($t = 21944 t_A$) of the core crash sawtooth are shown in Figure 2. The pressure distribution in our simulation is almost the same as the experimental observations (e.g., Fig. 2(b) in Reference [32]). In the present paper, we mainly focus on the time scale of the pressure crash.

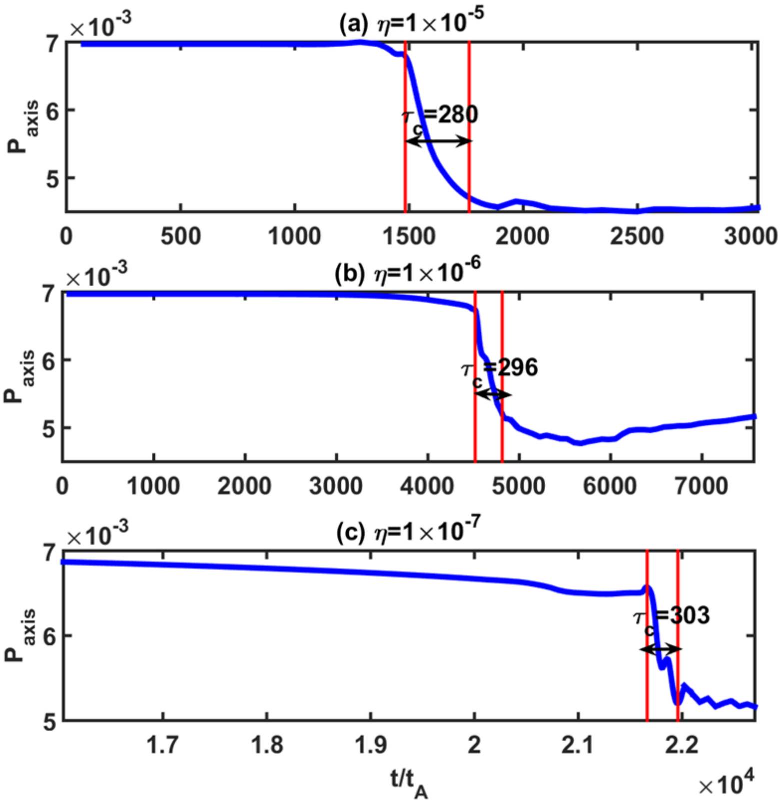

Figure 3 Evolution of the plasma pressure at the magnetic axis (P_{axis}) with η=1×10^{-5}, η=1×10^{-6}, and η=1×10^{-7}. The plasma pressure at the magnetic axis experiences a long time of very slow decrease phase and then exhibits a sudden crash for all cases.

Evolutions of the plasma pressure at the magnetic axis with η=1×10^{-5}, η=1×10^{-6}, and η=1×10^{-7} are shown in Figure 3. As we can see, the behaviors of pressure evolution are qualitatively the same for different η. At first, the plasma pressure at the magnetic axis almost remains unchanged for a long time, then experiences a very slow decay phase, and subsequently exhibits a sudden crash for all cases. In order to examine the speed of the pressure crash, the crash time is defined as the duration in which the decreasing rate of the plasma pressure at the magnetic axis is higher than 1.0×10^{-6}, i.e., $dp_{axis}/dt > 1.0\times10^{-6}$ (as illustrated in Figure 8). The crash time is in good agreement with the crash time directly estimated from Figure 3. Figure 4 shows the crash times for different resistivities (η=3×10^{-5}, η=1×10^{-5},

η=3×10^{-6}, η=1×10^{-6}, η=3×10^{-7}, and η=1×10^{-7}). It indicates that, although the pressure crashes associated with DTMs under different resistivities happen at different times, the crash time τ_c only slightly increases with decreasing η, i.e., $\tau_c \sim \eta^{-0.019}$. The dependence of the crash time on the resistivity is much weaker than both the Sweet-Parker reconnection $\tau_{SP} \sim \eta^{-1/2}$ [32] and the flow driven reconnection $\tau_R \sim \eta^{-1/5}$ [38]. According to the scaling law $\tau_c \sim \eta^{-0.019}$, for TFTR parameters ($\eta$~1×10^{-9}), the crash time $\tau_c \sim 331\tau_A \sim 36\mu s$, which is just in the range of TFTR observations (20~40 μs).[32]

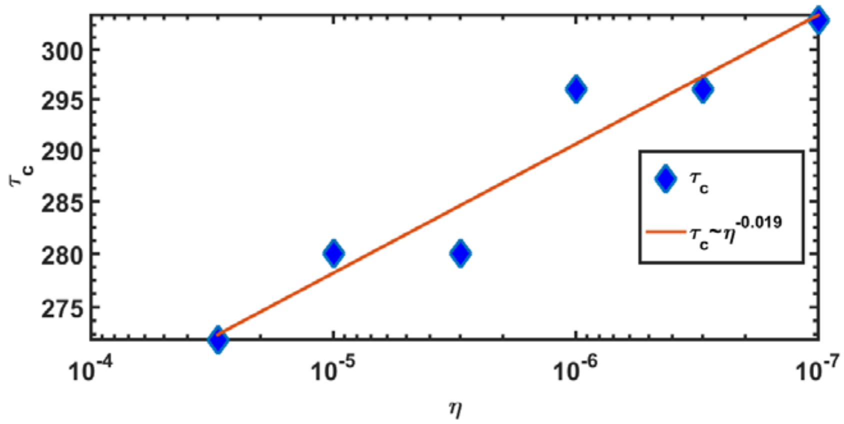

Figure 4 The crash time (τ_c) for the resistivity η=3×10^{-5}, η=1×10^{-5}, η=3×10^{-6}, η=1×10^{-6}, η=3×10^{-7}, and η=1×10^{-7}. The dependence of τ_c on the resistivity is $\tau_c \sim \eta^{-0.019}$, which is much weaker than that in previous studies.

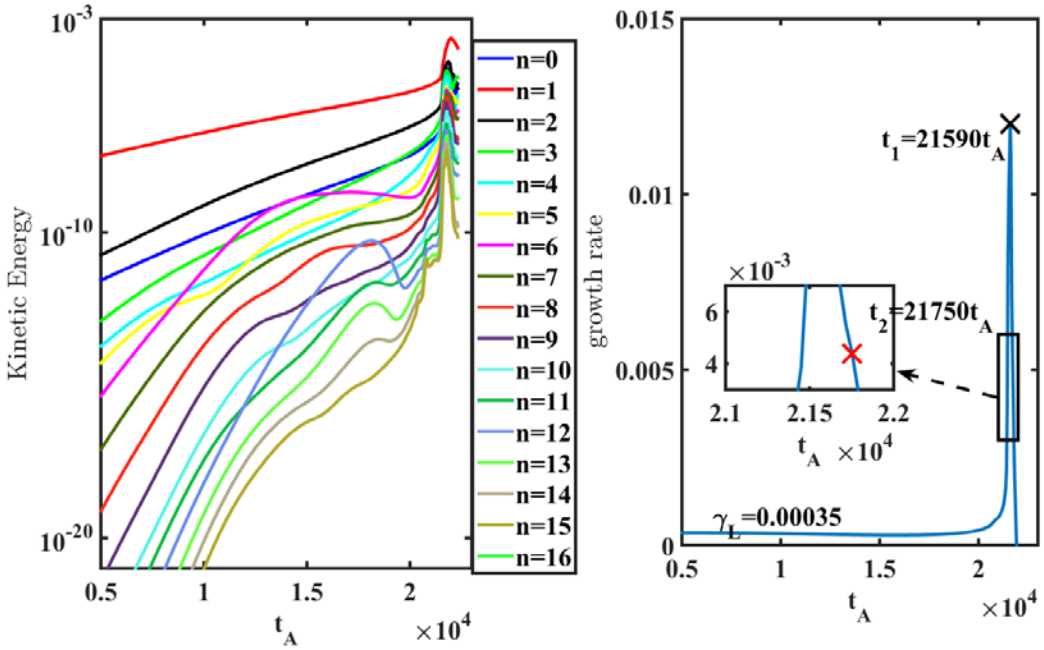

Figure 5 Evolutions of the kinetic energy for different toroidal numbers and the growth rate of total kinetic energy. The linear growth rate is $\gamma_L = 0.00035$ and the maximum nonlinear growth rate $\gamma_{\max} = 0.012$ at $t_1 \sim 21590 t_A$ (marked with a black '×'). The fastest pressure crash occurs at $t_2 \sim 21750 t_A$ (marked with a red '×'), which is about $160 t_A$ after the modes reach their peak growth rates.

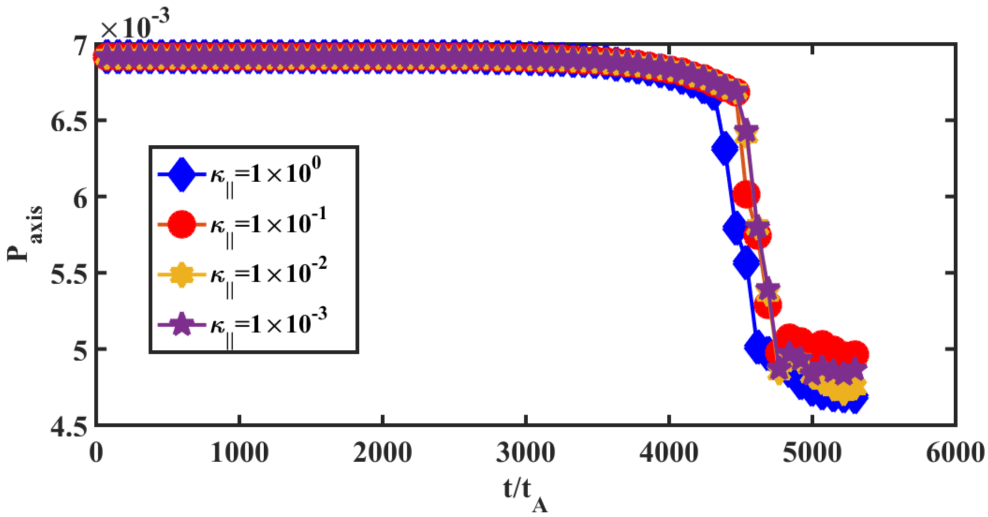

Figure 6 Pressure evolutions with $\eta = 1\times10^{-6}$ and different $\kappa_{\parallel}$.

The evolutions of the kinetic energy for different toroidal numbers and the growth rate of the total kinetic energy are shown in Figure 5. All mode amplitudes experience a long time of the slow linear growth phase, and then suddenly exhibits an explosive nonlinear growth before the fast pressure crash at $t \sim 21750 t_A$. The linear growth rate of total kinetic energy is $\gamma_L = 0.00035$, but the nonlinear growth rate quickly increases almost two orders of magnitude, $\gamma_{\max} = 0.012$. Such explosive growth of kinetic energy results from the nonlinear mode-mode coupling effect between the modes with different toroidal mode numbers.[47] However, it should be noted that the crash of the pressure does not happen in the explosive growth phase. As shown in Figure 5, the pressure crash begins at least $\sim 70 t_A$ and the fastest pressure crash takes place at about $160 t_A$ after the modes reach the maximum growth rate. Since the pressure crash time only takes about $280 t_A$, the time difference $\Delta t = 160 t_A$ for the maximum growth rate and the fastest pressure crash is unneglectable. Since the explosive growth of the modes is the result of the fast magnetic reconnection, the time difference between the peak growth rate and the fast crash indicates that the fast pressure crash is not directly resulted from the pressure diffusion along reconnected field lines. If the fast pressure crash is associated with parallel pressure diffusion, the time scales of the pressure crash should strongly depend on the parallel thermal conductivity. However, as shown in Figure 6, the pressure crash times for $\kappa_{\parallel}$ from 1×10^{-3} to 1 are almost the same (about $300 t_A$).

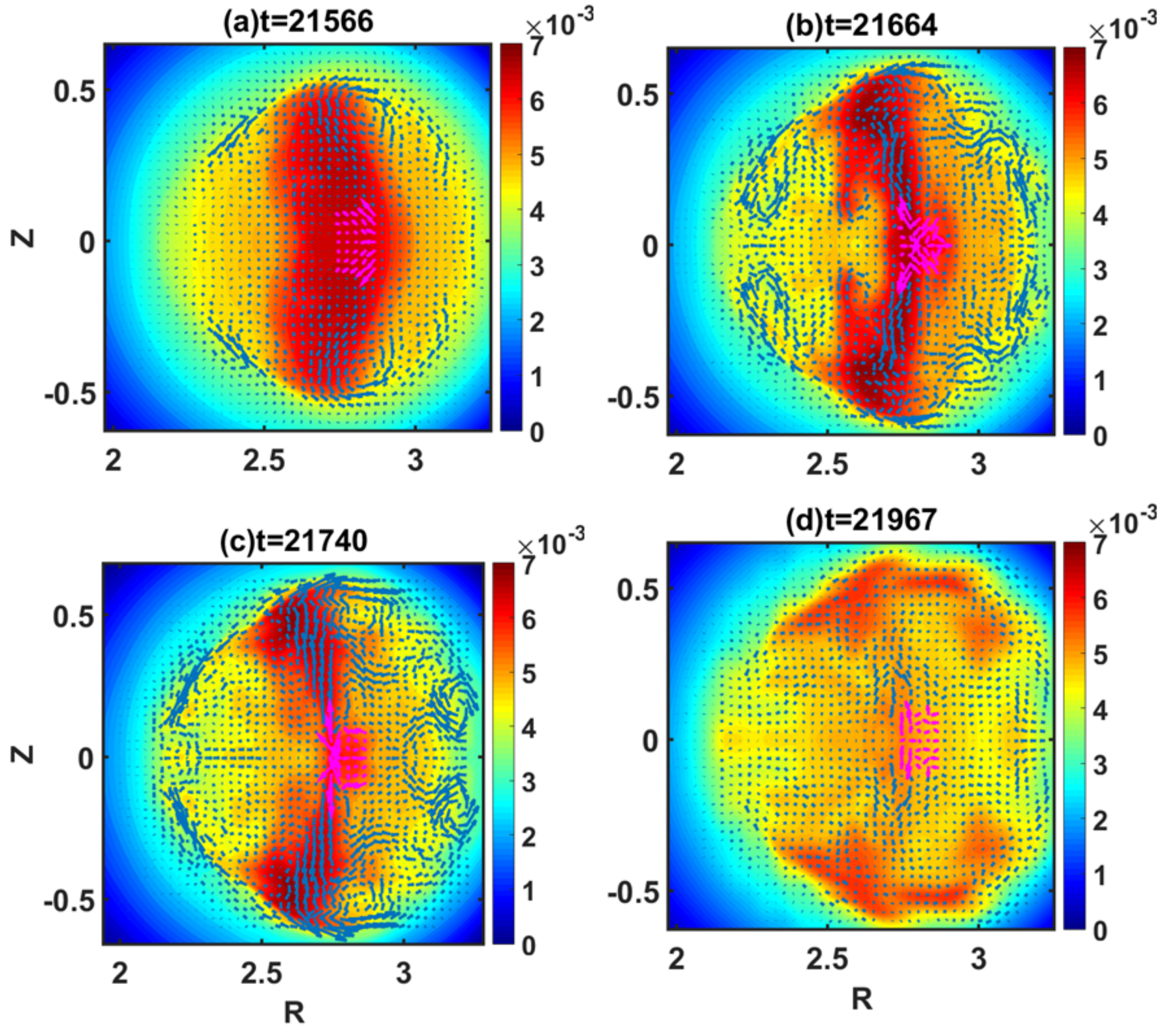

Figure 7 Snapshots of flow patterns (the arrows) and pressure distributions (the contour plots) (a) at the *m/n*=2/1 DTM precursor ($t = 21566t_A$), (b) at the beginning of the pressure crash ($t = 21664t_A$), (c) in the middle of the fastest crash ($t = 21740t_A$), (d) at the post-crash ($t = 21967t_A$). (These stages are also labeled in Figure 8.) The arrows marked with pink are the flows around the magnetic axis, which is mainly responsible for pressure crash at the magnetic axis. The velocities in each figure are normalized with the maximum value of the velocity in Figure 7(c).

In the previous studies, it is suggested that the fast pressure crash results from the explosive mode growth. But our results indicate that it is not the case because the crash of the core pressure takes place at about $160t_A$ after the modes reach their maximum growth rates. To further investigate the mechanism of the fast pressure crash, we inspect the flow patterns (the arrows) and pressure distributions (the contour plots) (a) at the *m/n*=2/1 DTM precursor ($t = 21566t_A$), (b) at the beginning of the pressure crash ($t = 21664t_A$), (c) in the middle of the fastest crash ($t = 21740t_A$), (d) at the post-crash ($t = 21967t_A$) as shown in Figure 7. During the development of DTM, the outer cold islands continuously grow and expand inward while the inner hot islands keep shrinking and been squeezed outward, which can also be seen from the Poincare plots of the magnetic field (Figure 2(c) and (e)). Therefore, the hot plasma core naturally becomes narrow and elongated, and a large pressure gradient is built up, as shown in Figure 2(d) and 7(a). Consequently, a strong radial flow is generated in the narrow and elongated hot region (Figure 7b and c). The radial flow can effectively transfer the hot plasma around the magnetic axis to the cold outer region. Then the evolution of the plasma pressure at the magnetic axis can be estimated by

$$\frac{\mathrm{d}p_{axis}}{dt} = (p_{axis} - p_{cold}) \times \frac{u_{out}}{L}, \tag{7}$$

where p_{axis} and p_{cold} are the plasma pressures at the magnetic axis and the outer region, respectively. u_{out} is the outward radial velocity of the magnetic axis and L is the spatial scale. Note that the pressure exchange occurs in the whole mixed region, then the spatial scale $L \sim a$. The detailed pressure evolution during the pressure crash and the corresponding dp_{axis}/dt measured in the simulation and the dp_{axis}/dt estimated by Eq. (7) are shown in Figure 8. During the DTM precursor, there is no radial flow near the magnetic axis. Therefore, P_{axis} remains almost unchanged. At the beginning of the nonlinear stage, the two outer islands begin to squeeze the inner core. As a result, P_{axis} slightly increases. As this effect could not be included in Eq. (7), the estimated dp_{axis}/dt differs from that of the simulation at this stage. However, after the fast crash begins, the two curves agree well with each other, especially for the first stage of the pressure crash. It indicates that the pressure crash at the magnetic axis is mainly due to the outward radial flow, and the time scale can be estimated by the outward radial flow velocity (i. e. $\tau_c \sim a / v_{out}$). To enssure this is validated, we have also carried out a series of simulations with different resistivities. It is found that the resistivity only affects when the narrow and elongated hot region forms, before the fast pressure crash starts. However, the influence of the resistivity on the crash time is feeble.

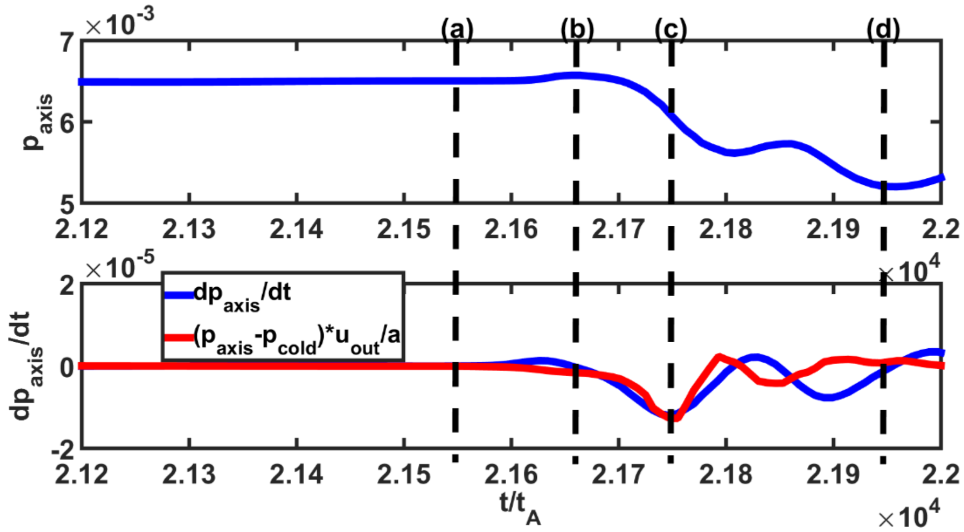

Figure 8 The detailed pressure evolution during pressure crash and the corresponding dp_{axis} / dt measured in simulation and the dp_{axis} / dt estimated by Eq. (7).

As discussed above, the generation of the radial flow is crucial for the fast pressure crash. However, it is still not clear how such a kind of radial flow could be generated. As we know, the plasma is usually frozen in the magnetic field, and it is impossible to generate a strong radial flow that moves across field lines. The possible reason is that flux surfaces in the core region are destroyed, and magnetic field lines become stochastic.

The mode structures with $n = 1,2,3$ and $m = 0 \sim 7$ (a) before the pressure crash at $t = 18085 t_A$ and (b) during the pressure crash at $t = 21694 t_A$ are shown in Figure 9. It is different from the DTM precursor that (1) all modes are well expanded in the whole core region during the pressure crash, which indicates the spatial broadening of the modes and (2) during plasma pressure crash the primary mode ($m/n = 2/1$) is not the dominant mode anymore, i.e., the maximum amplitudes of several higher *m* and *n* modes are comparable to the $m/n = 2/1$ mode. The energy spectrum (a) before the pressure crash at $t = 18085t_A$ and (b) during the pressure crash at $t = 21694t_A$ are shown in Figure 10. As we can see, the higher *n* modes gain notable energy during the pressure crash. For the *n*=1 and 2 modes, the amplitudes of the higher m modes (m>3) slightly increase only, but the spatial structures are largely broadened; however, for the $n \geq 3$ modes, they are not only broadened in the spatial space but also in the Fourier space. Since the modes become flattenning both in the real space and in the Fourier space, magnetic flux surfaces are totally destroyed and magnetic field lines become stochastic (Figure 2.c). That is why a strong radial flow from the magnetic axis to the outer could be generated.

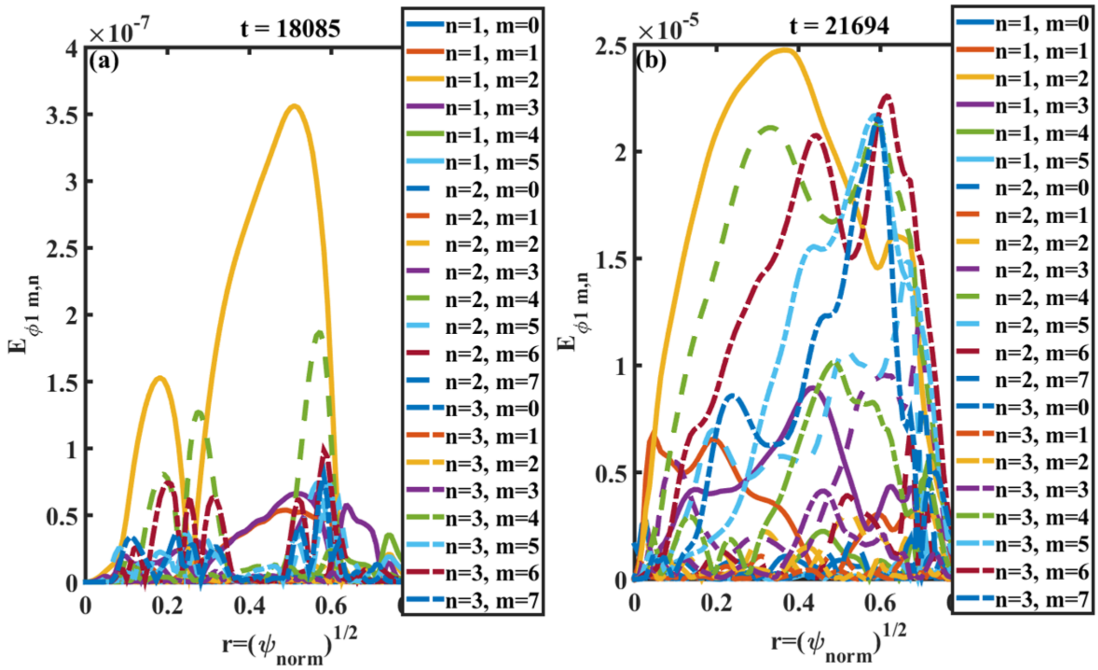

Figure 9 Mode structures of the modes with $n = 1, 2, 3$ and $m = 0 \sim 7$ (a) before the pressure crash at $t = 18085t_A$ and (b) during the pressure crash at $t = 21694t_A$.

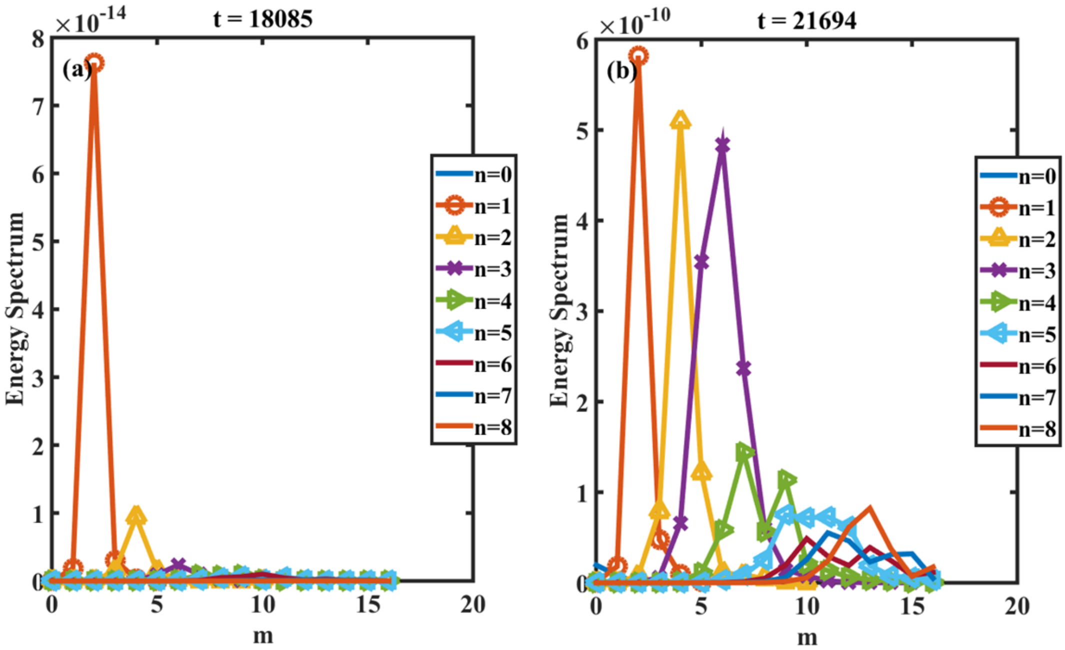

Figure 10 Energy spectrum (a) before the pressure crash at $t = 18085t_A$ and (b) during the pressure crash at $t = 21694t_A$.

As discussed above, these numerical simulations can explain the fast pressure crashes observed in TFTR.[32] However, could such a kind of MHD activity occur in other Tokamaks? Is it related to the geometry of Tokamak? To address this issue, we have also carried out numerical simulations with the geometry of EAST [49, 50] that is largely different from TFTR. The geometry of EAST is given as follows: the major radius $R_0 = 1.85m$, the minor radius $a = 0.45m$, the elongation E=1.9, and the triangularity $\sigma = 0.5$. All other parameters are the same as Section III.A. The pressure evolutions with $\eta=3\times10^{-5}$, $\eta=3\times10^{-6}$ and $\eta=3\times10^{-7}$ are shown in Figure 11. The crashes times are $\tau_c = 430t_A$, $\tau_c = 457t_A$, and $\tau_c = 483t_A$, respectively. The dependence of the pressure crash time on resistivity is $\tau_c \sim \eta^{-0.025}$ (Figure 12), which is qualitatively the same with Figure 4. It should be noted that the normalized Alfvén time in these cases is $t_A = 5.3\times10^{-8}s$ and the real crash time for $\eta=3\times10^{-7}$ is

$\tau_c = 483t_A \sim 26\mu s$. The flow patterns and contour plots of the pressure are shown in Figure 13. It is clear that, during the pressure crash, a strong radial flow is generated, and it can quickly transfer the hot plasma around the magnetic axis to the cold outer region. Although the EAST has the elongation E=1.9 and the triangularity $\sigma = 0.5$,which is largely different from TFTR[2], the results are qualitatively the same. It is indicated that such a kind of fast pressure crash could occur in different Tokamaks.

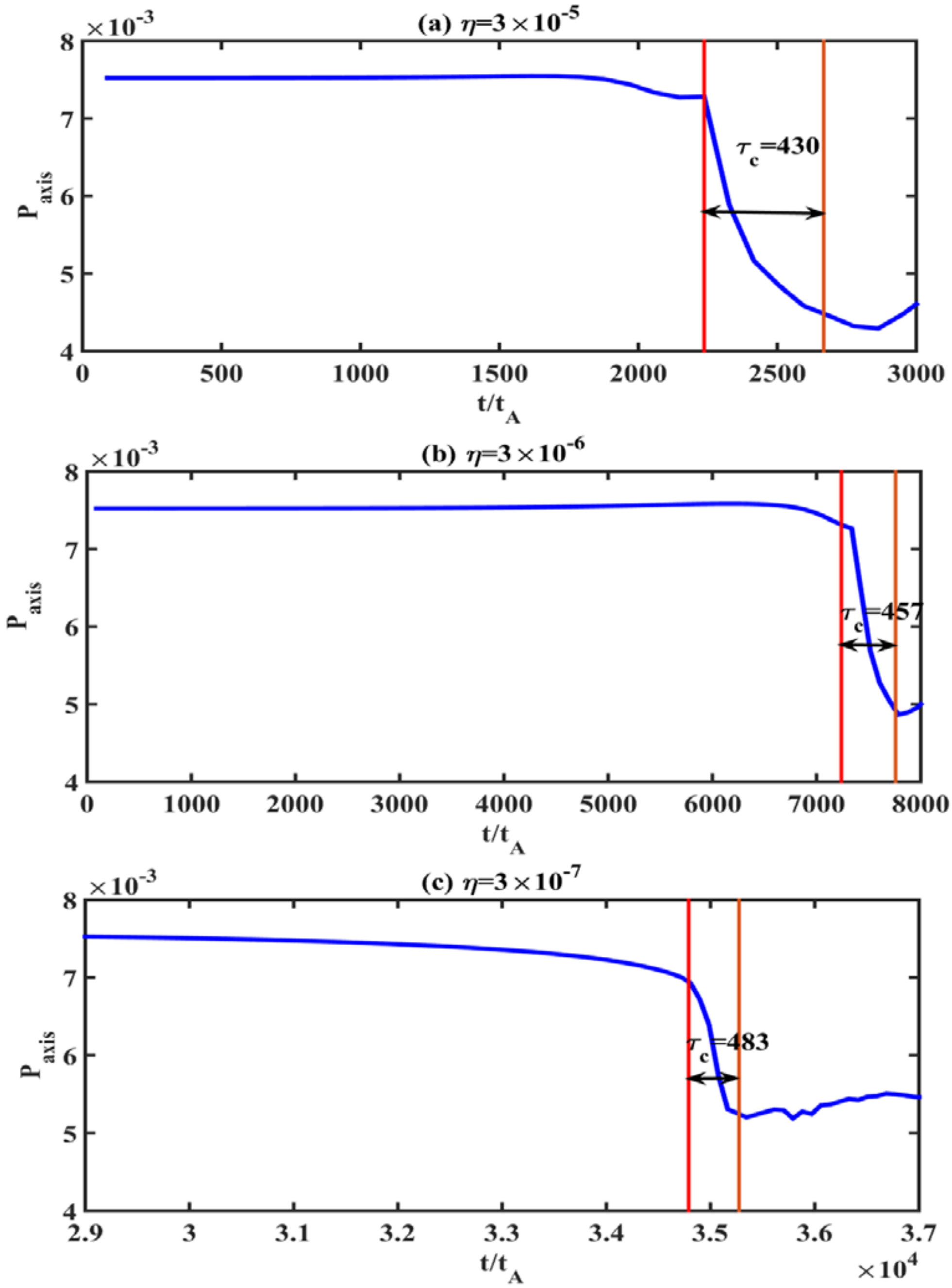

Figure 11 Pressure evolutions with $\eta=3\times10^{-5}$, $\eta=3\times10^{-6}$ and $\eta=3\times10^{-7}$

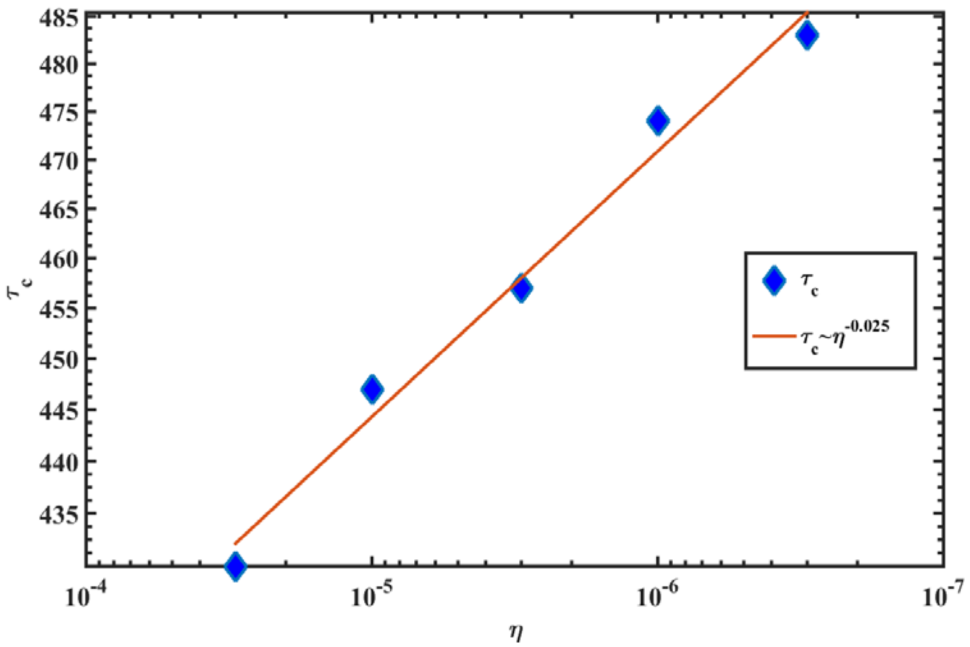

Figure 12 The crash time (τ_c) for the resistivity $\eta=3\times10^{-5}$, $\eta=1\times10^{-5}$, $\eta=3\times10^{-6}$, $\eta=1\times10^{-6}$, and $\eta=3\times10^{-7}$. The dependence of τ_c on the resistivity is $\tau_c \sim \eta^{-0.025}$, which is qualitatively the same with Figure 4.

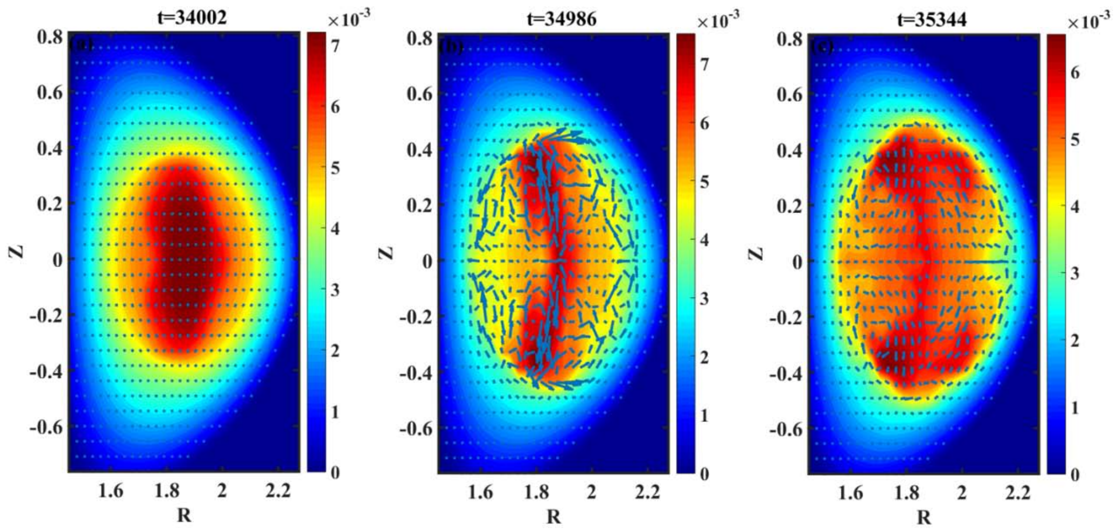

Figure 13 Snapshots of flow patterns (the arrows) and pressure distributions (the contour plots) (a) at the m/n=2/1 DTM precursor ($t=34002t_A$), (b) in the middle of the fast crash ($t=34986t_A$), (d) at the post-crash ($t=35344t_A$).The velocities in each figure are normalized with the maximum value of the velocity in Figure 13(b).

IV. Summary

A series of simulation studies of the fast pressure crash associated with the nonlinear evolution of the $m/n = 2/1$ DTM is carried out by using a three-dimensional toroidal and nonlinear MHD code CLT. It is found that the crash time of the plasma pressure at the magnetic axis is nearly independent of the resistivity. The crash time for typical TFTR parameters is about 36 μs, which is consistent with experimental observations (20~40 μs). [32]

In previous studies[34, 36, 38, 47], the fast pressure crash is supposed to result from the explosive growth of DTM. However, in the present paper, we find that the fast pressure crash at the magnetic axis does not happen in the explosive growth phase. Instead, it takes place at about $160t_A$ after the mode reaches the maximum growth rate. At this moment, the explosive growth almost finishes. It is also found that the crash time is independent of the parallel thermal conductivity, which also indicates that the pressure crash is not directly resulted from the fast reconnection. During the explosive growth, all modes with different *m* and *n* grow up, and the mode structures exhibit largely radial expansion. With many modes with different helicities well developed in the core region, flux surfaces are destroyed, and magnetic field lines become stochastic. Consequently, a strong radial flow from the hot magnetic core to cold plasma is generated and then quickly transfers the hot plasma around the magnetic axis to the outer region, resulting in the fast pressure crash.

The possible influence of the geometry of Tokamaks is also studied. It is found that such a kind of fast pressure crash is independent of a Tokamak geometry. The fast crash could happen in different Tokamaks and may also be related to the MHD activities observed in other Tokamaks (e. g. ASDEX-U[33] and Rijnhuizen Tokamak [51])

Acknowledgment

This work is supported by the National Natural Science Foundation of China under Grant No. 11775188 and 11835010, the Special Project on High-performance Computing under the National Key R&D Program of China No. 2016YFB0200603, Fundamental Research Fund for Chinese Central Universities.

Reference

[1] E.J. Strait, L.L. Lao, M.E. Mauel, B.W. Rice, T.S. Taylor, K.H. Burrell, M.S. Chu, E.A. Lazarus, T.H. Osborne, S.J. Thompson, A.D. Turnbull, Enhanced Confinement and Stability in DIII-D Discharges with Reversed Magnetic Shear, Physical Review Letters, 75 (1995) 4421-4424.

[2] F.M. Levinton, M.C. Zarnstorff, S.H. Batha, M. Bell, R.E. Bell, R.V. Budny, C. Bush, Z. Chang, E. Fredrickson, A. Janos, J. Manickam, A. Ramsey, S.A. Sabbagh, G.L. Schmidt, E.J. Synakowski, G. Taylor, Improved Confinement with Reversed Magnetic Shear in TFTR, Physical Review Letters, 75 (1995) 4417-4420.

[3] H.Y. Yuh, S.M. Kaye, F.M. Levinton, E. Mazzucato, D.R. Mikkelsen, D.R. Smith, R.E. Bell, J.C. Hosea, B.P. LeBlanc, J.L. Peterson, H.K. Park, W. Lee, Suppression of Electron Temperature Gradient Turbulence via Negative Magnetic Shear in NSTX, Physical Review Letters, 106 (2011) 055003.

[4] E. Joffrin, C.D. Challis, G.D. Conway, X. Garbet, A. Gude, S. Günter, N.C. Hawkes, T.C. Hender, D.F. Howell, G.T.A. Huysmans, E. Lazzaro, P. Maget, M. Marachek, A.G. Peeters, S.D. Pinches, S.E. Sharapov, J.-E. contributors, Internal transport barrier triggering by rational magnetic flux surfaces in tokamaks, Nuclear Fusion, 43 (2003) 1167-1174.

[5] M. Hugon, B.P.v. Milligen, P. Smeulders, L.C. Appel, D.V. Bartlett, D. Boucher, A.W. Edwards, L.G. Eriksson, C.W. Gowers, T.C. Hender, G. Huysmans, J.J. Jacquinot, P. Kupschus, L. Porte, P.H. Rebut, D.F.H. Start, F. Tibone, B.J.D. Tubbing, M.L. Watkins, W. Zwingmann, Shear reversal and MHD activity during pellet enhanced performance pulses in JET, Nuclear Fusion, 32 (1992) 33-43.

[6] C. Kessel, J. Manickam, G. Rewoldt, W.M. Tang, Improved plasma performance in tokamaks with negative magnetic shear, Physical Review Letters, 72 (1994) 1212-1215.

[7] A. Sykes, J.A. Wesson, S.J. Cox, High-$\ensuremath{\beta}$ Tokamaks, Physical Review Letters, 39 (1977) 757-760.

[8] A.C.C. Sips, O. for the Steady State, A. the Transport Physics topical groups of the International Tokamak Physics, Advanced scenarios for ITER operation, Plasma Physics and Controlled Fusion, 47 (2005) A19.

[9] R. Aymar, P. Barabaschi, Y. Shimomura, The ITER design, Plasma Physics and Controlled Fusion, 44 (2002) 519.

[10] Y.X. Wan, J.G. Li, Y. Liu, X.L. Wang, C. Vincent, C.G. Chen, X.R. Duan, P. Fu, X. Gao, K.M. Feng, S.l. Liu, Y.T. Song, P.D. Weng, B.N. Wan, F.R. Wan, H.Y. Wang, S.T. Wu, M.Y. Ye, Q.W. Yang, G.Y. Zheng, G. Zhuang, Q. Li, C. team, Overview of the present progress and activities on the CFETR, Nuclear Fusion, 57 (2017) 102009.

[11] B. Carreras, H.R. Hicks, B.V. Waddell, Tearing-mode activity for hollow current profiles, Nuclear Fusion, 19 (1979) 583.

[12] P.L. Pritchett, Y.C. Lee, J.F. Drake, Linear analysis of the double-tearing mode, The Physics of Fluids, 23 (1980) 1368-1374.

[13] J.W. Connor, S.C. Cowley, R.J. Hastie, T.C. Hender, A. Hood, T.J. Martin, Tearing modes in toroidal geometry, The Physics of Fluids, 31 (1988) 577-590.

[14] L. Ofman, Double tearing instability with shear flow, Physics of Fluids B: Plasma Physics, 4 (1992) 2751-2757.

[15] M. Taro, N. Hiroshi, T. Shinji, K. Yasuaki, Nonlinear behaviour of collisionless double tearing mode induced by electron inertia, Nuclear Fusion, 45 (2005) 1264.

[16] P. Maget, H. Lütjens, J.-F. Luciani, X. Garbet, O. Février, J.-L. Ségui, Bi-fluid and neoclassical effect on a Double-Tearing mode in Tore Supra, Physics of Plasmas, 21 (2014) 062504.

[17] Q. Yu, S. Günter, Numerical modelling of neoclassical double tearing modes, Nuclear Fusion, 39 (1999) 487.

[18] L. Wei, Z.-X. Wang, Nonlinear evolution of double tearing modes in tokamak plasmas via multiple helicity simulation, Nuclear Fusion, 54 (2014) 043015.

[19] L. Wei, Z.-X. Wang, A mode transition in self-suppressing double tearing modes via Alfvén resonance in rotating tokamak plasmas, Nuclear Fusion, 51 (2011) 123005.

[20] A. Mao, J. Li, J. Liu, Y. Kishimoto, Zonal flow dynamics in the double tearing mode with antisymmetric shear flows, Physics of Plasmas, 21 (2014) 052304.

[21] Y. Ishii, A.I. Smolyakov, M. Takechi, Plasma rotation effects on magnetic island formation and the trigger of disruptions in reversed shear plasma, Nuclear Fusion, 49 (2009) 085006.

[22] T. Liu, Z.X. Wang, J.L. Wang, L. Wei, Suppression of explosive bursts triggered by neo-classical tearing mode in reversed magnetic shear tokamak plasmas via ECCD, Nuclear Fusion, 58 (2018) 076026.

[23] E. Fredrickson, M. Bell, R.V. Budny, E. Synakowski, Nonlinear evolution of double tearing modes in tokamaks, Physics of Plasmas, 7 (2000) 4112-4120.

[24] W. Guo, J. Ma, Q. Yu, Numerical study on nonlinear growth of m/n = 3/1 double tearing mode in high Lundquist number regime, Plasma Physics and Controlled Fusion, 61 (2019) 075011.

[25] L. Wang, W.B. Lin, X.Q. Wang, Effects of resonant magnetic perturbation on the triggering and the evolution of double-tearing mode, EPL (Europhysics Letters), 121 (2018) 45001.

[26] J. Wang, Z.X. Wang, L. Wei, Y. Liu, Control of neo-classical double tearing modes by differential poloidal rotation in reversed magnetic shear tokamak plasmas, Nuclear Fusion, 57 (2017) 046007.

[27] J. Ma, W. Guo, Z. Yu, Q. Yu, Effect of plasmoids on nonlinear evolution of double tearing modes, Nuclear Fusion, 57 (2017) 126004.

[28] T. Akramov, H. Baty, Non-linear growth of double tearing mode: Explosive reconnection, plasmoid formation, and particle acceleration, Physics of Plasmas, 24 (2017) 082116.

[29] T. Liu, J.F. Yang, G.Z. Hao, Y.Q. Liu, Z.X. Wang, S. Zheng, A.K. Wang, H.D. He,

Multiple MHD instabilities in high- β N toroidal plasmas with reversed magnetic shear, Plasma Physics and Controlled Fusion, 59 (2017) 065009.

[30] G. Sun, C. Dong, L. Duan, Effects of electron cyclotron current drive on the evolution of double tearing mode, Physics of Plasmas, 22 (2015) 092509.

[31] J. Pétri, M. Takamoto, H. Baty, S. Zenitani, Explosive reconnection of the double tearing mode in relativistic plasmas with application to the Crab nebula, Plasma Physics and Controlled Fusion, 57 (2014) 014034.

[32] Z. Chang, W. Park, E.D. Fredrickson, S.H. Batha, M.G. Bell, R. Bell, R.V. Budny, C.E. Bush, A. Janos, F.M. Levinton, K.M. McGuire, H. Park, S.A. Sabbagh, G.L. Schmidt, S.D. Scott, E.J. Synakowski, H. Takahashi, G. Taylor, M.C. Zarnstorff, Off-Axis Sawteeth and Double-Tearing Reconnection in Reversed Magnetic Shear Plasmas in TFTR, Physical Review Letters, 77 (1996) 3553-3556.

[33] S. Günter, S. Schade, M. Maraschek, S.D. Pinches, E. Strumberger, R. Wolf, Q. Yu, A.U. Team, MHD phenomena in reversed shear discharges on ASDEX Upgrade, Nuclear Fusion, 40 (2000) 1541.

[34] Y. Ishii, M. Azumi, Y. Kishimoto, Structure-Driven Nonlinear Instability of Double Tearing Modes and the Abrupt Growth after Long-Time-Scale Evolution, Physical Review Letters, 89 (2002) 205002.

[35] Y. Ishii, M. Azumi, Y. Kishimoto, J.N. Leboeuf, Long timescale plasma dynamics and explosive growth driven by the double tearing mode in reversed shear plasmas, Nuclear Fusion, 43 (2003) 539.

[36] M. Janvier, Y. Kishimoto, J.Q. Li, Structure-Driven Nonlinear Instability as the Origin of the Explosive Reconnection Dynamics in Resistive Double Tearing Modes, Physical Review Letters, 107 (2011) 195001.

[37] A. Bierwage, S. Hamaguchi, M. Wakatani, S. Benkadda, X. Leoncini, Nonlinear Evolution of $q=1$ Triple Tearing Modes in a Tokamak Plasma, Physical Review Letters, 94 (2005) 065001.

[38] Z.X. Wang, X.G. Wang, J.Q. Dong, Y.A. Lei, Y.X. Long, Z.Z. Mou, W.X. Qu, Fast Resistive Reconnection Regime in the Nonlinear Evolution of Double Tearing Modes, Physical Review Letters, 99 (2007) 185004.

[39] Y. Ishii, M. Azumi, G. Kurita, T. Tuda, Nonlinear evolution of double tearing modes, Physics of Plasmas, 7 (2000) 4477-4491.

[40] C.L. Zhang, Z.W. Ma, Nonlinear evolution of double tearing mode in Hall magnetohydrodynamics, Physics of Plasmas, 16 (2009) 122113.

[41] M. Janvier, Y. Kishimoto, J. Li, Critical parameters for the nonlinear destabilization of double tearing modes in reversed shear plasmas, Nuclear Fusion, 51 (2011) 083016.

[42] C.L. Zhang, Z.W. Ma, Nonlinear evolution of double tearing mode with guiding magnetic field, Physics of Plasmas, 18 (2011) 052303.

[43] C.L. Zhang, Z.W. Ma, J.Q. Dong, A Simulation Study of Hall Effect on Double Tearing Modes, Plasma Science and Technology, 10 (2008) 407.

[44] E.N. Parker, Sweet's mechanism for merging magnetic fields in conducting fluids, Journal of Geophysical Research, 62 (1957) 509-520.

[45] X.G. Wang, Z.W. Ma, A. Bhattacharjee, Fast magnetic reconnection and sudden

enhancement of current sheets due to inward boundary flows, Physics of Plasmas, 3 (1996) 2129-2134.

[46] S. Wang, Z. Ma, Influence of toroidal rotation on resistive tearing modes in tokamaks, Physics of Plasmas, 22 (2015) 122504.

[47] W. Zhang, Z.W. Ma, J. Zhu, H.W. Zhang, Core-crash sawtooth associated with <i>m/n</i>=2/1 double tearing mode in Tokamak, Plasma Physics and Controlled Fusion, (2019).

[48] C. Cheng, M. Chance, NOVA: A nonvariational code for solving the MHD stability of axisymmetric toroidal plasmas, Journal of Computational Physics, 71 (1987) 124-146.

[49] B.N. Wan, Y.F. Liang, X.Z. Gong, J.G. Li, N. Xiang, G.S. Xu, Y.W. Sun, L. Wang, J.P. Qian, H.Q. Liu, X.D. Zhang, L.Q. Hu, J.S. Hu, F.K. Liu, C.D. Hu, Y.P. Zhao, L. Zeng, M. Wang, H.D. Xu, G.N. Luo, A.M. Garofalo, A. Ekedahl, L. Zhang, X.J. Zhang, J. Huang, B.J. Ding, Q. Zang, M.H. Li, F. Ding, S.Y. Ding, B. Lyu, Y.W. Yu, T. Zhang, Y. Zhang, G.Q. Li, T.Y. Xia, Overview of EAST experiments on the development of high-performance steady-state scenario, Nuclear Fusion, 57 (2017) 102019.

[50] B.N. Wan, Y. Liang, X.Z. Gong, N. Xiang, G.S. Xu, Y. Sun, L. Wang, J.P. Qian, H.Q. Liu, L. Zeng, L. Zhang, X.J. Zhang, B.J. Ding, Q. Zang, B. Lyu, A.M. Garofalo, A. Ekedahl, M.H. Li, F. Ding, S.Y. Ding, H.F. Du, D.F. Kong, Y. Yu, Y. Yang, Z.P. Luo, J. Huang, T. Zhang, Y. Zhang, G.Q. Li, T.Y. Xia, Recent advances in EAST physics experiments in support of steady-state operation for ITAB, Nuclear Fusion, 59 (2019) 112003.

[51] M.R. de Baar, G.M.D. Hogeweij, N.J. Lopes Cardozo, A.A.M. Oomens, F.C. Schüller, Electron Thermal Transport Barrier and Magnetohydrodynamic Activity Observed in Tokamak Plasmas with Negative Central Shear, Physical Review Letters, 78 (1997) 4573-4576.